Diffusion of chemically reactive species in stagnation point flow of a micropolar viscoelastic fluid in a porous medium over a stretching/shrinking sheet

Z. Abbas^{a,*}, M. Sheikh^a, and M. Sajid^b

^{a}*Department of Mathematics, The Islamia University of Bahawalpur,*
Bahawalpur 63100, Pakistan,
**Tel.: +92 62 9255480;*
e-mail: za_qau@yahoo.com
^{b}*Department of Mathematics and Statistics, International Islamic University,*
Islamabad 44000, Pakistan.

The transfer of chemically reactive species in stagnation point flow of a laminar micropolar viscoelastic fluid immersed in a porous medium over a stretching/shrinking surface is considered. The reactive species diffused into the fluid from the surface undergo a one stage isothermal and homogenous reaction. A similarity transformation is employed to transform the developed partial differential equations into a system of coupled ordinary differential equations. A convergent series solution is developed using homotopy analysis method in the whole spatial region ($0 \leq \eta \leq \infty$). The obtained solutions for velocity, microrotation and concentration of species are analysed for various emerging parameters through graphs and tables.

1. Introduction

It is well known phenomena that traditional Newtonian fluid is inadequate to describe the characteristics of fluid with suspended particles. The non-Newtonian fluid that incorporates the motion of suspended particles is the micropolar fluid. Micropolar fluids consist of randomly oriented dumb-bell shaped particles that can undergo a rotation. Some examples of such fluids are colloidal fluids, biological fluids, polymeric fluids, liquid crystal and exotic lubricants etc. The rotation of these particles affects the overall dynamics of the flow phenomena. Eringen [1] first derived the governing equations of micropolar fluids and later extended it to the theory of thermomicropolar fluids [2]. In flow equations describing micropolar fluid phenomena, the principle of conservation of angular momentum is essential along with the standard equations for the conservation of mass and momentum. The details regarding the theory of micropolar fluids can be seen in the book by Lukaszewics [3]. The theory of micropolar viscoelastic is established for such problems in which the typical theory of viscoelastic is unavailable due to microstructure in the substance. Generally, these problems are related to grain bodies and multimolecular materials like polymer. Eringen [4] constructed the linear theory of micropolar viscoelasticity. McCarthy and Eringen [5] studied the propagation of waves in micropolar viscoelastic medium. Saint-Venant's principle of micropolar viscoelastic substances was described by DeCicco and Nappa [6]. Kumar [7] presented the wave propagation in micropolar viscoelastic generalized thermoelastic solid. For application point of view, one can study Kumar and Choudhary [8] in which they investigated the dynamic problem in micropolar viscoelastic medium.

Diffusion of chemically reactive species into the fluid from the surface is another important area of research in recent years. The applications of such process include polymer production, manufacture of ceramics and glassware, food processing etc. Chambre and Young [9] investigated the diffusion of chemical reactive species in a laminar boundary layer flow. The problem discussed in Ref. 9 was extended for a stretching sheet by Anderson *et al.* [10]. Mohamed and Abo-Dahab [11] investigated the influence of chemical reaction and thermal radiation in a MHD micropolar fluid. They also incorporated the effects of porous medium. The effect of MHD, mass transfer and chemical reaction in a second grade fluid flowing through a porous medium over a stretching sheet was discussed by Cortell [12]. In another paper, Cortell [13] presented the numerical solution for two classes of viscoelastic fluids with chemically reacting species. A literature survey reveals that different aspects of flow have been investigated under the diffusion of chemically reactive species. Das *et al.* [14] presented the effects of homogeneous first order chemical reaction on the flow past an impulsively started plate. Muthucumaraswamy [15,16] respectively investigated the influence of chemical reaction on the flow past an impulsively started vertical plate with uniform heat and mass flux without and with suction. The problem of wedge flow with suction and injection and chemical reaction has been considered by Devi and Kandasamy [17]. The further details of influence of chemically reacting species on different flow situations can be seen in the literature [18-25]. Stagnation point flow of viscoelastic fluid has been investigated by Beard and Walters [26]. They have obtained a perturbation solution of problem up to first order. The problem of stagnation point flow in a micropolar fluid was studied by Nazar *et*

al. [27]. A literature survey reveals that stagnation point flow has been investigated for a range of non-Newtonian fluids, for example see Xu *et al.* [28], Hayat *et al.* [29], Abbas *et al.* [30], Sajid *et al.* [31], Yacob *et al.* [32], Hayat *et al.* [33], Mosta *et al.* [34], Nandy [35] and many references there in. In a study El-Kabir [36] combined the effects of micropolar and viscoelastic fluids and discussed the hydromagnetic stagnation point flow in a micropolar viscoelastic fluid. In a recent paper Abbas *et al.* [37] discussed the heat transfer analysis in a micropolar viscoelastic fluid past a stretching/shrinking sheet in the presence of magnetic field.

The objective of the present paper is to study the stagnation point flow of micropolar viscoelastic fluid past a stretching/shrinking sheet immersed in a porous medium with chemically reactive species. In this problem for viscoelastic fluid, we considered the Walters' B model. The problem is formulated using nth-order homogeneous chemical reaction of constant rate k_n. With the help of suitable transformations the governing partial differential equations are converted to ordinary differential equations and then solved analytically using homotopy analysis method.

2. Formulation of the problem

Consider a steady, incompressible and two-dimensional stagnation-point flow of a micropolar viscoelastic fluid embedded in a porous medium due to a stretching/shrinking surface at $y = 0$ the flow covers the region $y > 0$. The sheet is stretched/shrunk in the x-direction so that the x-component of velocity is $u_w(x) = bx$ where $b > 0$ and $b < 0$ are for stretching and shrinking cases, respectively. It is also assumed that the velocity of the external flow is given by $u_\infty(x) = ax$, where $a > 0$ is the strength of the stagnation flow. By assuming c_w and c_∞. As the concentrations at the wall and far away from the sheet, respectively, mass transfer analysis is also carried out. Following Eringen [4], El-Kabeir [36] and Muhaimin *et al.* [38], the basic governing boundary layer equations of micropolar viscoelastic fluid and concentration field in the absence of body forces are:

$$\frac{\partial u}{\partial x} + \frac{\partial v}{\partial y} = 0, \tag{1}$$

$$u\frac{\partial u}{\partial x} + v\frac{\partial u}{\partial y} = a^2 x + \left(\nu + \frac{k_1}{\rho}\right)\frac{\partial^2 u}{\partial y^2}$$
$$+ \frac{k_1}{\rho}\frac{\partial N}{\partial y} + \frac{\nu}{k}(ax - u) - k^*\left(u\frac{\partial^3 u}{\partial x \partial y^2}\right.$$
$$\left. + v\frac{\partial^3 u}{\partial y^3} + \frac{\partial u}{\partial x}\frac{\partial^2 u}{\partial y^2} - \frac{\partial u}{\partial y}\frac{\partial^2 u}{\partial x \partial y}\right), \tag{2}$$

$$u\frac{\partial N}{\partial x} + v\frac{\partial N}{\partial y} = \frac{\gamma}{\rho j}\frac{\partial^2 N}{\partial y^2} - \frac{k_1}{\rho j}\left(2N + \frac{\partial u}{\partial y}\right), \tag{3}$$

$$u\frac{\partial c}{\partial x} + v\frac{\partial c}{\partial y} = D\frac{\partial^2 c}{\partial y^2} - k_n c^n, \tag{4}$$
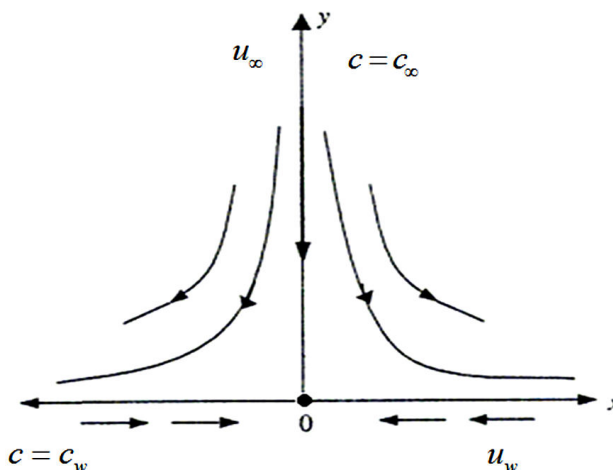

FIGURE 1. Physical model and coordinate system.

here u and v are the velocity components in the x- and y-axis directions, respectively, ν is the fluid kinematic viscosity, k_1 is the vortex viscosity, ρ is the fluid density, N is the micro-rotation or angular velocity, k is the permeability of the porous medium, k^* is the Weissenberg number, γ is the spin gradient viscosity and j is the microinertia per unit mass, whereas c is the concentration of the fluid, D is the diffusion coefficient and k_n is the n th-order chemical reaction rate constant.

It is clear from Eq. (2) that the order of partial differential equation is higher than the Navier-Stokes equations. Therefore, one needs an additional boundary condition. Garg and Rajagopal [39] proposed the idea of augmenting the boundary condition at the free stream.

Implementing the same here, we have the following boundary conditions for the present flow:

$$u = u_w(x) = bx, \quad v = 0,$$

$$N = -m_0\frac{\partial u}{\partial y}, \quad \text{at} \quad y = 0, \tag{5}$$

$$u = u_\infty(x) = ax, \quad \frac{\partial u}{\partial y} \to 0, N = 0,$$

$$c \to c_\infty \quad \text{as} \quad y \to \infty, \tag{6}$$

where 'a' and 'b' both are constant having dimension (time)$^{-1}$ and m_0 ($0 \le m_0 \le 1$) is a constant. Whereas, $m_0 = 0$ represents that the concentrated particle flow where the microelements near the wall surface are not able to rotate (*i.e.* $N = 0$). This situation is called strong concentration of microelements [40]. However, $m_0 = 1/2$ implies the vanishing of anti-symmetric part of the stress tensor and known as weak concentration of microelements [41]. Here in this problem we just take into account the case of $m_0 = 0$.

We use the following non-dimensionalize variables to simplify the flow problem

$$\eta = \sqrt{\frac{a}{\nu}}y, \quad u = axf'(\eta), \quad v = -\sqrt{a\nu}f(\eta),$$

$$N = \sqrt{\frac{a}{\nu}}axg(\eta), \quad c = c_w\phi(\eta). \tag{7}$$

With the help of Eq. (7), the continuity Eq. (1) is identically satisfied and Eqs. (2-4) take the form

$$(1+k)f'' + Kg' + ff'' + 1 - f'^2 + \lambda(1 - f')$$
$$- k_0(2f'f'' - f''^2 - f^{iv}) = 0 \tag{8}$$

$$\left(1 + \frac{K}{2}\right)g'' - K(2g + f'') - f'g + g'f = 0, \tag{9}$$

$$\phi'' + Scf\phi' = Sc\gamma\phi^n, \tag{10}$$

subject to the boundary conditions

$$f = 0 \quad f' = \frac{b}{a} = \varepsilon, \quad g = -m_0f''(0),$$

$$\phi = 1 \quad \text{at} \quad \eta = 0, \tag{11}$$

$$f' = 1, \quad f'' = 0, \quad g = 0, \quad \text{at} \quad \eta \to \infty. \tag{12}$$

where a prime is a differentiation with respect to η, $k = k_1/\rho v$ is the micropolar parameter, $k_0 = ak^*/v\rho$ is the viscoelastic parameter, $\lambda = v/ka$ is the porosity parameter, $Sc = v/D$ is the Schmidt number, $\gamma = k_nc_w^{n-1}/a$ is the chemical reaction rate parameter (it must be a real number while $\gamma < 0$ denotes generative chemical reaction and $\gamma > 0$ indicates destructive chemical reaction and we take $\gamma = 0$ for non-reactive species, see [12,42]. It is further noted that for $n \neq 1$, the chemical reaction rate parameter represents the nth order chemical reaction and for $n = 1$ it reduces to the first-order chemical reaction) and $\varepsilon > 0$ for a stretching sheet, $\varepsilon < 0$ for a shrinking sheet and $\varepsilon = 0$ for a static sheet.

It is evident from Eq. (13) that the highest derivative term has a coefficient k_0f which is zero at $\eta = 0$ and when $k_0 \to 0$ i.e. for a viscous micropolar fluid. Therefore, due to singularity at the starting point of the domain the numerical solution is not straight forward.

The wall shear stress is defined as

$$C_f = \frac{\tau_w}{\rho u_\infty^2}$$

$$\tau_w = \left[(\mu + k_1)\left(\frac{\partial u}{\partial y}\right) - k^*\left(u\frac{\partial^2 u}{\partial x\partial y}\right.\right.$$

$$\left.\left. + v\frac{\partial^2 u}{\partial y^2} + 2\frac{\partial u}{\partial x}\frac{\partial u}{\partial y}\right) + k_1N\right]_{y=0},$$

$$= \rho ax\sqrt{a\nu}\big[(1+K)f''(0) - k_0(3f'(0)f''(0)$$

$$- f(0)f'''(0)) + Kg(0)\big],$$

$$= \rho ax\sqrt{a\nu}\big[(1+K)f''(0) - k_0(3f'(0)f''(0))\big]$$

$$C_f\sqrt{Re_x} = (1+K)f''(0) - k_0(3f'(0)f''(0)). \tag{13}$$

The wall couple stress is defined as

$$M_x = \frac{m_w}{\rho a^2 x^3}, \quad m_w = \gamma\left(\frac{\partial N}{\partial y}\right)_{y=0},$$

$$M_xRe_x = KGg'(0), \tag{14}$$

in which $G = G_1a/v$ is the microrotation parameter and $G_1 = \gamma/k_1$ is the microrotation constant.

The Sherwood number is defined as

$$Sh_x = \frac{xj_w}{D(c_w - c_\infty)}, \quad j_w = -D\left(\frac{\partial c}{\partial y}\right)_{y=0},$$

$$\frac{Sh_x}{\sqrt{Re_x}} = -\phi'(0), \tag{15}$$

where $Re_x = ax^2/v$ is a local Reynolds number.

3. Homotopy analysis solution

Homotopy analysis method is used to get the series solutions of the non-linear boundary value problems consisting of Eqs. (8)-(10) with boundary conditions (11) and (12). The set of base functions for fluid velocity $f(\eta)$ angular velocity $g(\eta)$ and concentration field $\phi(\eta)$ can be defined as

$$\left\{\eta^k\exp(-n\beta\eta)|k \geq 0, \beta > 0\right\} \tag{16}$$

in the form

$$f(\eta) = a_{0,0}^0 + \sum_{n=0}^{\infty}\sum_{k=0}^{\infty}a_{m,n}^k\eta^k\exp(-n\beta\eta), \tag{17}$$

$$g(\eta) = b_{0,0}^0 + \sum_{n=0}^{\infty}\sum_{k=0}^{\infty}b_{m,n}^k\eta^k\exp(-n\beta\eta), \tag{18}$$

$$\phi(\eta) = \sum_{n=0}^{\infty}\sum_{k=0}^{\infty}c_{m,n}^k\eta^k\exp(-n\beta\eta), \tag{19}$$

here $a_{m,n}^k$, $b_{m,n}^k$ and $c_{m,n}^k$ are the coefficients and $\beta > 0$ is a scale parameter. By the rule of solution expressions of $f(\eta)$, $g(\eta)$ and $\phi(\eta)$ as well as through the support of boundary conditions (11) and (17) we are able to select $f_0(\eta)$, $g_0(\eta)$ and $\phi_0(\eta)$ as the initial guess approximations of $f(\eta)$, $g(\eta)$ and $\phi(\eta)$

$$f_0(\eta) = \eta + \frac{\varepsilon - 1}{\beta}(1 + e^{-\beta\eta}), \tag{20}$$

$$g_0(\eta) = 0, \tag{21}$$

$$\phi_0(\eta) = e^{-\beta\eta}, \tag{22}$$

and the auxiliary linear operators

$$L_f(f) = \frac{\partial^3 f}{\partial \eta^3} - \beta^2 \frac{\partial f}{\partial \eta}, \qquad (23)$$

$$L_g(f) = \frac{\partial^3 f}{\partial \eta^3} - \beta^2 f, \qquad (24)$$

$$L_\phi(f) = \frac{\partial^2 f}{\partial \eta^2} - \beta^2 f, \qquad (25)$$

that satisfy the following properties

$$L_f \left[C_1 + C_2 \exp(-\beta\eta) + c_3 \exp(\beta\eta) \right] = 0, \qquad (26)$$

$$L_g \left[C_4 \exp(-\beta\eta) + c_5 \exp(\beta\eta) \right] = 0, \qquad (27)$$

$$L_\phi \left[C_6 \exp(-\beta\eta) + c_7 \exp(\beta\eta) \right] = 0, \qquad (28)$$

where $C_i (i = 1, 2, 3, 45, 6, 7)$ are arbitrary constants, which can be determined using boundary conditions (11) and (12).

The zeroth-order deformation problems are constructed as follows:

$$(1-q)L_f \left[\widehat{f}(\eta; q) - f_0(\eta) \right] = q\hbar_f N_f \left[\widehat{f}(\eta; q) \right] \qquad (29)$$

$$(1-q)L_g \left[\widehat{g}(\eta; q) - g_0(\eta) \right] = q\hbar_g N_g \left[\widehat{g}(\eta; q) \right] \qquad (30)$$

$$(1-q)L_\phi \left[\widehat{\phi}(\eta; q) - \phi_0(\eta) \right] = q\hbar_\phi N_\phi \left[\widehat{\phi}(\eta; q) \right] \qquad (31)$$

$$\widehat{f}(0, q) = 0, \quad \frac{\partial \widehat{f}(0; q)}{\partial \eta} = \varepsilon, \quad \widehat{g}(0, q) = -m_0 \frac{\partial^2 \widehat{f}(0; q)}{\partial \eta^2},$$

$$\widehat{\phi}(0, q) = 1, \quad \frac{\partial \widehat{f}(\infty; q)}{\partial \eta} = 1 \qquad (32)$$

$$\frac{\partial \widehat{f}(\infty; q)}{\partial \eta} = 1, \quad \frac{\partial^2 \widehat{f}(\infty; q)}{\partial \eta^2} = 0,$$

$$\widehat{g}(\infty, q) = 0, \quad \widehat{\phi}(\infty, q) = 0, \qquad (33)$$

where $q \in [0, 1]$ is an embedding parameter and $\hbar_f$, $\hbar_g$ and $\hbar_\phi$ denote the non-zero auxiliary parameters, the non-linear operators N_f, N_g and N_ϕ are

$$N_f[\widehat{f}(\eta, q)] = (1+K)\frac{\partial^3 \widehat{f}(\eta, q)}{\partial \eta^3} + K\frac{\partial \widehat{g}(\eta, q)}{\partial \eta} + \widehat{f}(\eta, q)\frac{\partial^2 \widehat{f}(\eta, q)}{\partial \eta^2} + 1 - \left(\frac{\partial \widehat{f}(\eta, q)}{\partial \eta} \right)^2$$

$$+ \lambda \left(1 - \frac{\partial \widehat{f}(\eta, q)}{\partial \eta} \right) - k_0 \left\{ \begin{array}{c} 2\frac{\partial \widehat{f}(\eta,q)}{\partial \eta}\frac{\partial^3 \widehat{f}(\eta,q)}{\partial \eta^3} - \widehat{f}(\eta, q)\frac{\partial^4 \widehat{f}(\eta,q)}{\partial \eta^4} \\ - \left(\frac{\partial^2 \widehat{f}(\eta,q)}{\partial \eta^2} \right)^2 \end{array} \right\} \qquad (34)$$

$$N_g[\widehat{g}(\eta, q)] = \left(1 + \frac{K}{2} \right) \frac{\partial^2 \widehat{g}(\eta, q)}{\partial \eta^2} - K \left(2g + \frac{\partial^2 \widehat{f}(\eta, q)}{\partial \eta^2} \right) + \widehat{f}(\eta, q)\left(\frac{\partial \widehat{g}(\eta, q)}{\partial \eta} \right) - \widehat{g}(\eta, q)\frac{\partial \widehat{f}(\eta, q)}{\partial \eta}, \qquad (35)$$

$$N_\phi[\widehat{\phi}(\eta, q)] = \frac{\partial^2 \widehat{\phi}(\eta, q)}{\partial \eta^2} + Sc\widehat{f}(\eta, q)\frac{\partial \widehat{\phi}(\eta, q)}{\partial \eta} - Sc\gamma(\widehat{\phi}(\eta, q))^n. \qquad (36)$$

The above zeroth-order Eqs. (29)-(31) possess following solutions for $q = 0$ and $q = 1$

$$\widehat{f}(\eta; 0) = f_0(\eta), \quad \widehat{f}(\eta; 1) = f(\eta) \qquad (37)$$

$$\widehat{g}(\eta; 0) = g_0(\eta), \quad \widehat{g}(\eta; 1) = g(\eta) \qquad (38)$$

$$\widehat{\phi}(\eta; 0) = \phi_0(\eta), \quad \widehat{\phi}(\eta; 1) = \phi(\eta) \qquad (39)$$

By using Taylor's series with regard to q we get

$$\widehat{f}(\eta, q) = f_0(\eta) + \sum_{m-1}^{\infty} f_m(\eta)q^m, \qquad (40)$$

$$\widehat{g}(\eta, q) = g_0(\eta) + \sum_{m-1}^{\infty} g_m(\eta)q^m, \qquad (41)$$

$$\widehat{\phi}(\eta, q) = \phi_0(\eta) + \sum_{m-1}^{\infty} \phi_m(\eta)q^m, \qquad (42)$$

here

$$f_m(\eta) = \frac{1}{m!}\frac{\partial^m \widehat{f}(\eta; q)}{\partial q^m}\bigg|_{q=0},$$

$$g_m(\eta) = \frac{1}{m!}\frac{\partial^m \widehat{g}(\eta; q)}{\partial q^m}\bigg|_{q=0},$$

$$\phi_m(\eta) = \frac{1}{m!}\frac{\partial^m \widehat{\phi}(\eta; q)}{\partial q^m}\bigg|_{q=0}. \qquad (43)$$

For the convergence of the series solutions, the values of $\hbar_f$, $\hbar_g$ and $\hbar_\phi$ are selected in such a way that at $q = 1$ the given series are convergent and finally the series solutions are of the form:

$$f(\eta) = f_0(\eta) + \sum_{m-1}^{\infty} f_m(\eta), \qquad (44)$$

$$g(\eta) = g_0(\eta) + \sum_{m-1}^{\infty} g_m(\eta), \qquad (45)$$

$$\phi(\eta) = \phi_0(\eta) + \sum_{m=1}^{\infty} \phi_m(\eta). \tag{46}$$

For m th-order deformation equations, we simply differentiate the zeroth-order deformations Eqs. (29)-(31), m times with respect to embedding parameter then take $q = 0$ and finally dividing by $m!$ then we have

$$L_f[f_m(\eta) - \chi_m f_{m-1}(\eta)] = \hbar_f R_m^f(\eta), \tag{47}$$

$$L_g[g_m(\eta) - \chi_m g_{m-1}(\eta)] = \hbar_g R_m^g(\eta), \tag{48}$$

$$L_\phi[\phi_m(\eta) - \chi_m \phi_{m-1}(\eta)] = \hbar_\phi R_m^\phi(\eta), \tag{49}$$

$$f_m(0) = f_m'(0) = g_m(0) = \phi_m(0) = 0, \tag{50}$$

$$f_m'(\infty) = f_m''(\infty) = g_m(\infty) = \phi_m(\infty) = 0, \tag{51}$$

where

$$R_m^f(\eta) = (1 + K)f_{m-1}^m(\eta) + Kg_{m-1}'(\eta)$$
$$+ 1 + \lambda(1 - f_{m-1}^m(\eta))$$
$$+ \left[\begin{array}{c} f_{m-1-k} f_k'' - f_{m-1-k}' f_k' \\ -k_0(2f_{m-1-k}' f_k'' - f_{m-1-k} f_k^{iv} - f_{m-1-k}'' f_k'') \end{array} \right], \tag{52}$$

$$R_m^g(\eta) = \left(1 + \frac{K}{2}\right) g_{m-1}''(\eta) - K(2g_{m-1}(\eta)$$
$$+ f_{m-1}''(\eta)) + \sum_{k=0}^{m-1} [f_{m-1-k} g_k' - g_{m-1-k} f_k'], \tag{53}$$

$$R_m^\phi(\eta) = \phi_{m-1}''(\eta)$$
$$- Sc\gamma\phi_{m-1}^n(\eta) + \sum_{k=0}^{m-1} [f_{m-1-k} \phi_k'], \tag{54}$$

$$\chi_m = \begin{cases} 0, & m \le 1, \\ 1, & m > 1. \end{cases} \tag{55}$$

Let f_m^*, g_m^* and ϕ_m^* be the special functions of Eqs. (47)-(49) then the general solutions of Eqs. (47)-(49) are defined as

$$f_m(\eta) = f_m^*(\eta) + C_1 + C_2 \exp(-\beta\eta) + C_3 \exp(\beta\eta), \tag{56}$$

$$g_m(\eta) = g_m^*(\eta) + C_4 \exp(-\beta\eta) + C_5 \exp(\beta\eta), \tag{57}$$

$$\phi_m(\eta) = \phi_m^*(\eta) + C_6 \exp(-\beta\eta) + C_7 \exp(\beta\eta), \tag{58}$$
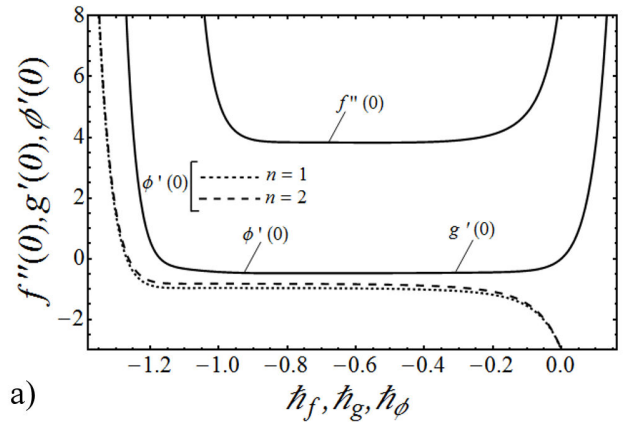
in which the values of constants $C_i(i = 1, 2, 3, 4, 5, 6, 7)$ are achieved through boundary conditions (50) to (51) as

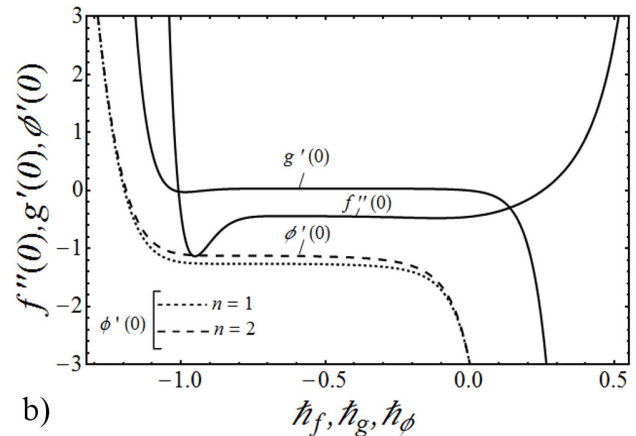$$C_2 = \frac{1}{\beta} \frac{\partial f_m^*(\eta)}{\partial \eta}\bigg|_{\eta=0},$$

$$C_1 = -C_2 - f_m^*(0), \quad C_3 = 0 \tag{59}$$

$$C_5 = -g_m^*(0), \quad C_4 = 0, \tag{60}$$

$$C_7 = -\phi_m^*(0), \quad C_6 = 0. \tag{61}$$

FIGURE 2. a) The $\hbar$ -curves of $f''(0)$, g$'(0)$ and $\phi'(0)$ at 20th-order of approximation for $k_0 = 0.5$, $K = 0.5$, $\lambda = 0.5$, $\beta = 3$, $Sc = 1$ and $\gamma = 1$ in the case of shrinking sheet. b) The $\hbar$ -curves of $f''(0)$, g$'(0)$ and $\phi'(0)$ at 20th-order of approximation for $k_0 = 0.5$, $K = 0.5$, $\lambda = 0.25$, $\beta = 3$, $Sc = 1$ and $\gamma = 1$ in the case of stretching sheet.

Using software Mathematica or any other, one might solve Eqs. (47)-(49) one after the other in the order $m = 1, 2, 3, 4 \ldots$

4. Convergence of HAM solution

By applying homotopy analysis method, the analytical solutions in the form of series must converge to the exact solution of original problem which is under consideration and it is already explained by Liao [43]. Many researchers [44-52] applied this method to solve highly non-linear problems. To ensure the convergence region and rate of approximation for the homotopy analysis method, the non-zero auxiliary parameters $\hbar_f$, $\hbar_g$ and $\hbar_\phi$ are chosen accurately by plotting the so-called $\hbar$-curves. In Figs. 2a and 2b, the $\hbar$-curves of $f''(0)$, g$'(0)$ and $\phi'(0)$ at 20th-order of approximation are shown. It is noted from these figures that $\hbar$-curves have parallel line segments that correspond to the region $-0.8 \le \hbar_g \le -0.3$, $-0.6 \le \hbar_f \le -0.1$ for $\hbar_f$, and for $\hbar_g$ the region is $-1 \le \hbar_g \le -0.1$ and $-0.7 \le \hbar_g \le 0$ respectively, for shrinking sheet and stretching sheet. Whereas, for $\hbar_\phi$ the region is

TABLE I. Values of $f''(0)$, $g'(0)$ and $\phi'(0)$ for different order of approximation when $k_0 = 0.5$, $K = 0.2$, $\lambda = 0.8$, $\beta = 3$, $S_c = 1.5$, $\gamma = 3$, $\hbar_f = \hbar_g = \hbar_\phi = -0.5$ and $\varepsilon = -0.25$.

Order of approximation	$f''(0)$	$G'(0)$	$\phi'(0)$	
			$n = 1$	$n = 2$
1	2.26202	-0.11796	-2.16084	-1.82570
5	2.02696	-0.13646	-2.13054	-1.76435
10	2.02682	-0.13647	-2.13053	-1.76450
15	2.02682	-0.13647	-2.13053	-1.76450
20	2.02682	-0.13647	-2.13053	-1.76450
30	2.02682	-0.13647	-2.13053	-1.76450
40	2.02682	-0.13647	-2.13053	-1.76450

FIGURE 4. Velocity profiles for various values of the porosity parameter λ and the micropolar parameter K with viscoelastic parameter $k_0 = 0.5$ and $\beta = 3$ in case of shrinking sheet.
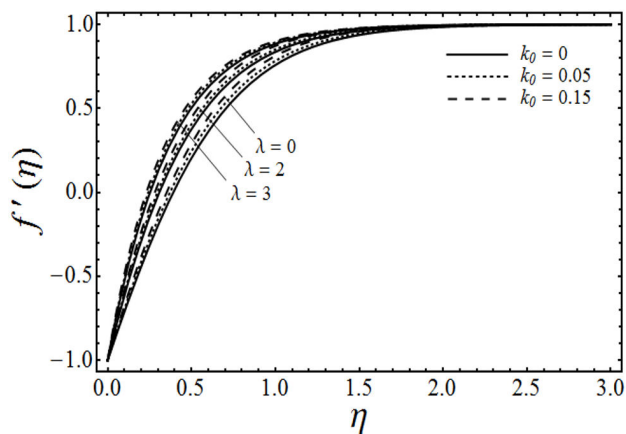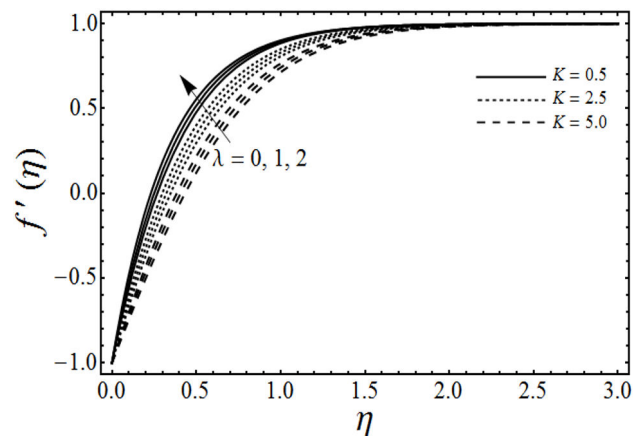

FIGURE 3. Velocity profiles for various values of the porosity parameter λ and the viscoelastic parameter k_0 with micropolar parameter $K = 0$ and $\beta = 3$ in case of shrinking sheet.
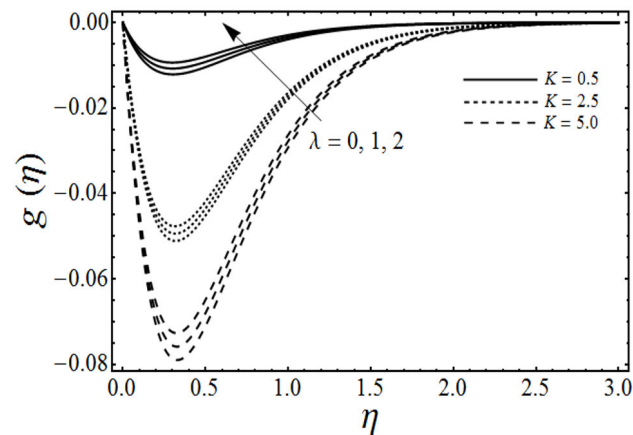

FIGURE 5. Microrotation profiles for various values of the porosity parameter λ and the micropolar parameter K with viscoelastic parameter $k_0 = 0.5$ and $\beta = 3$ in case of shrinking sheet.

$-1.2 \leq \hbar_\phi \leq -0.3$, $-1 \leq \hbar_\phi \leq -0.2$, respectively, for shrinking sheet and stretching sheet. For the convergence of HAM solution the values of the $\hbar$ greatly depend on the values of pertinent parameters. Table I is made to show the convergence of HAM solution for different order of approximations. From this table, one can see that after the 10th-order approximation, the given series solutions are convergent for velocity, microrotation velocity and concentration field.

5. Results and discussion

The non-linear boundary value problem consisting of Eqs. (8)-(10) with boundary conditions (11) and (12) is solved analytically by means of homotopy analysis method in the whole domain ($0 \leq \eta \leq \infty$) to compute the fluid velocity $f'(\eta)$, microrotation or angular velocity $g(\eta)$ and the concentration field $\phi(\eta)$. The fluid velocity component, angular velocity and the concentration profiles are plotted to observe the effects of the various involving parameters, for example the micropolar parameter K, porosity parameter λ, viscoelastic parameter k_0, Schmidt number Sc and chemical reaction rate parameter γ in Figs. (3)-(12). Furthermore, we

have computed and showed the numerical values of the skin-friction coefficient, wall couple stress and the Sherwood number for several physical parameters both graphically and in tabular form. The comparison of the present results with the existing results is given in limited cases, and we found them to be in excellent agreement.

Figure 3 shows the variation in the fluid velocity component $f'(\eta)$ for several values of a viscoelastic parameter k_0 and porosity parameter λ in the case of ($K = 0$) with β and ε fixed. From this Fig. 4, it is evident that the fluid velocity $f'(\eta)$ increases with an increase in both λ and k_0. Figure 4 gives the change in the fluid velocity component $f'(\eta)$ for various values of the porosity parameter λ and the micropolar parameter K (in the case of viscoelastic fluid $k_0 = 0.5$) by keeping β and ε fixed. It is found in figure that the fluid velocity increases with an increase in porosity parameter λ by keeping the values of K constant, but on the other side as we increase the values of micropolar parameter K the fluid velocity $f'(\eta)$ decreases. However with the increasing values of micropolar parameter K the momentum boundary layer
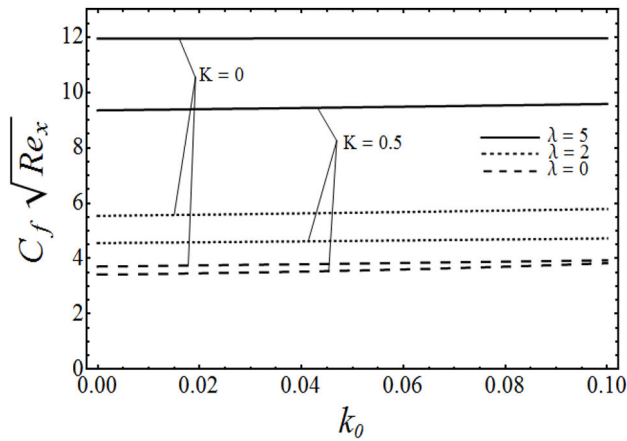
FIGURE 6. Variation of skin friction coefficient with the viscoelastic parameter k_0, for various values of micropolar parameter K and the porosity parameter λ with $\beta = 3$ in case of $\varepsilon = -1$.

thickness increases. Figure 5 elucidates the effects of the porosity parameter λ and the micropolar parameter K on the angular velocity $g(\eta)$ in case of viscoelastic fluid ($k_0 = 0.5$) with other parameters β and ε are fixed. From this figure we can see that the angular or microrotation velocity $g(\eta)$ goes to decrease by increasing the values of micropolar parameter K whereas it increases with an increase in porosity parameter λ. It is also noted from this figure that the angular velocity over shoot near the sheet due to a microrotation of the

fluid particles. Figure 6 gives the variation of the skin-friction coefficient $C_f \sqrt{Re_x}$ versus the viscoelastic parameter k_0 for several values of porosity parameter λ and micropolar parameter K with β and ε fixed. Fromo this figure, it is evident that the magnitude of the skin-friction coefficient increases with an increase in porosity parameter λ, whereas it decreases by increasing the values of micropolar parameter K. Figure 7 shows the change in the wall couple stress $M_x Re_x$ versus viscoelastic parameter k_0 for different values of micropolar parameter K and porosity parameter λ by keeping β and ε fixed. The magnitude of the wall couple stress or angular-velocity gradient at the wall is increased with an increase in K, λ and k_0.

The change in the concentration field $\phi(\eta)$ for different values of homogeneous chemical reaction rate n, viscoelastic parameter k_0 and micropolar parameter K in the case of destructive chemical reaction $\gamma = 2$ is presented in Fig. 8 keeping β and ε fixed. From this figure we can see that the concentration field $\phi(\eta)$ is increased with an increase in n and K, whereas it decreases by increasing the values of viscoelastic parameter k_0. Figure 9 shows the influence of the concentration field $\phi(\eta)$ for several values of porosity parameter λ and n in the case of destructive chemical reaction ($\gamma = 2$) by keeping K, k_0, S_c, β and ε fixed. It is observed from this figure that the concentration field is increased with an increase in both n and λ. Figure 10 gives the variation of the

TABLE II. Comparison of present results of wall shear stress $C_f \sqrt{Re_x}$ with the existing results in the case of Newtonian fluid ($K = k_0$ and $\lambda = 0$) for various values of ε (stretching/shrinking sheet).

| ε	Bhattacharyya et al. [53]	Wang [54]	Ishak et al. [55]	Rosali et al. [56]	Present results
-0.24	1.40224051	1.40224			1.40224
-0.50	1.49566948	1.49567			1.49567
-0.615	1.50724089				1.50724
-0.75	1.48929834	1.48930			1.48930
-1.00	1.32881689	1.32882			1.32926
-1.15	1.08223164	1.08223			1.08426
-1.20	0.93247243				0.94237
-1.2465	0.58429146	0.55430			0.73998
0		1.232588	1.232588	1.232588	1.23259
0.1		1.14656	1.146561	1.146561	1.14656
0.2		1.05113	1.051130	1.051130	1.05113
0.3				0.946816	0.946816
0.4				0.834072	0.834072
0.5		0.71330	0.713295	0.713295	0.713295
1		0.0	0.0	0.0	0.0
2		-1.88731	-1.887307	-1.887307	-1.88731
3			-4.276541	-4.276541	-4.27654
4			-7.086378	-7.086378	-7.08638
5		-10.26475	-10.264749	-10.264749	-10.2647
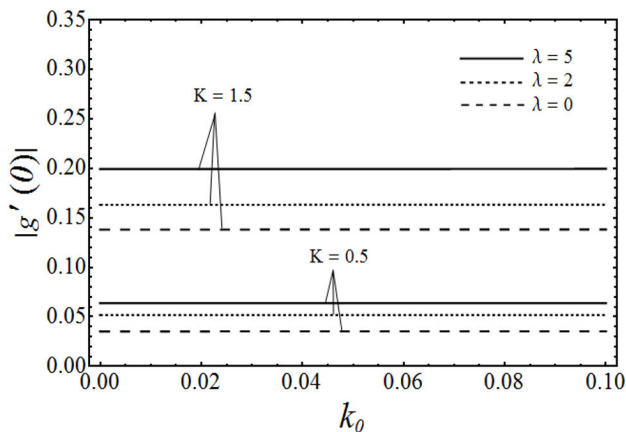
FIGURE 7. Variation of $|g'(0)|$, which is proportional to the wall couple stress, with the viscoelastic parameter k_0, for various values of the micropolar parameter K and the porosity parameter λ with $\beta = 3$ in case of $\varepsilon = -1$.
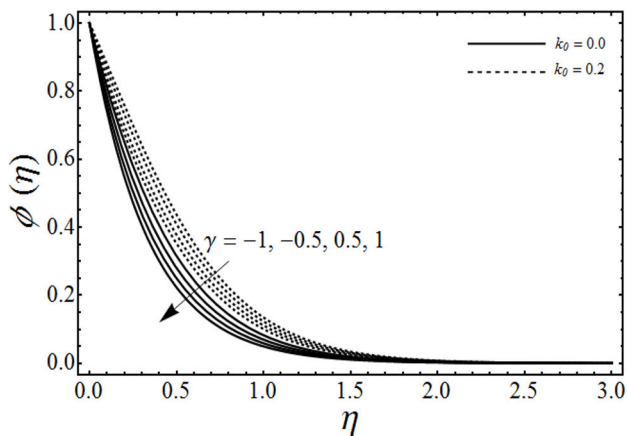

FIGURE 10. Concentration profiles for various values of the chemical reaction rate parameter γ and the viscoelastic parameter k_0 with porosity parameter $\lambda = 1$, micropolar parameter $k = 0.5$, Schmidt number $Sc = 2$, $\beta = 3$ and $n = 2$ in case of shrinking sheet.
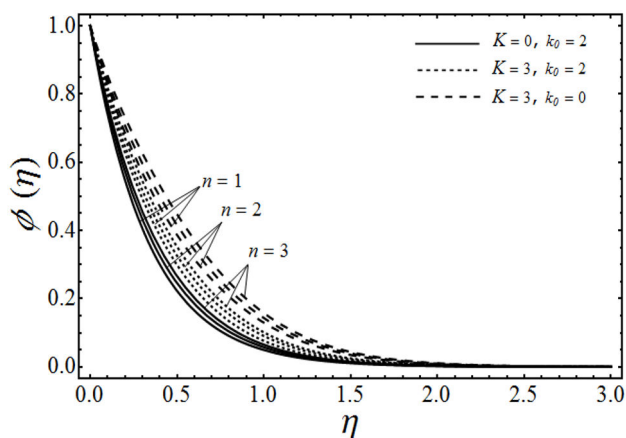

FIGURE 8. Concentration profiles for various values of the micropolar parameter K and the viscoelastic parameter k_0 with porosity parameter $\lambda = 1$ Schmidt number $Sc = 2$, chemical reaction rate parameter $\gamma = 2$ and $\beta = 3$ in case of shrinking sheet.
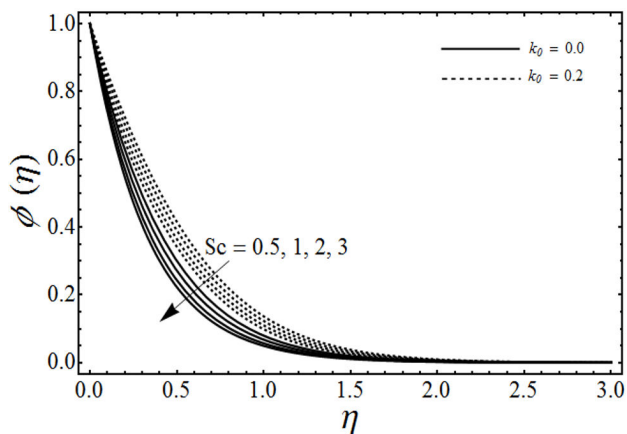

FIGURE 11. Concentration profiles for various values of the Schmidt number Sc and the viscoelastic parameter k_0 with porosity parameter $\lambda = 1$, micropolar parameter $K = 0.5$, chemical reaction rate parameter $\gamma = 2$, $\beta = 3$ and $n = 2$ in case of shrinking sheet.
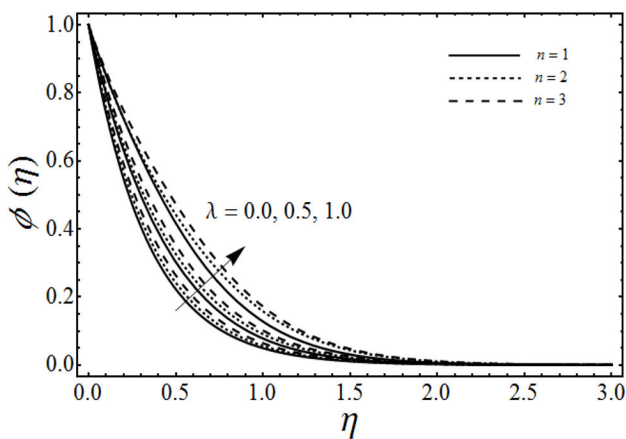
FIGURE 9. Concentration profiles for various values of porosity parameter λ with micropolar parameter $K = 3$, viscoelastic parameter $k_0 = 2$, Schmidt number $Sc = 2$, chemical reaction rate parameter $\gamma = 2$ and $\beta = 3$ in case of shrinking sheet.

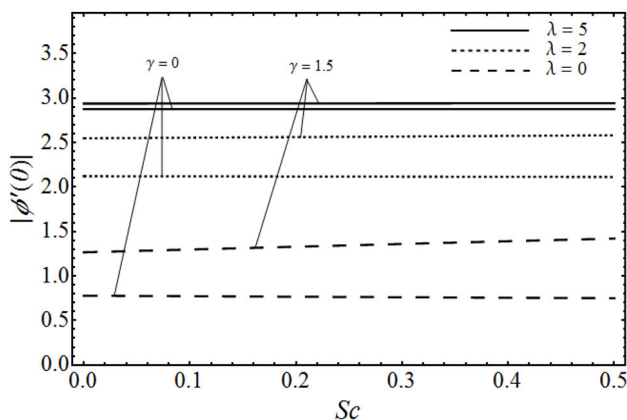FIGURE 12. Variation of $|\phi'(0)|$, for various values of the Schmidt number Sc and porosity parameter λ with the viscoelastic parameter $k_0 = 0.5$, the micropolar parameter $K = 0.5$ and $\beta = 3$ in case of $\varepsilon = -1$.

TABLE III. Comparison of present results of Sherwood number with the existing results in the case of Newtonian fluid for stretching sheet.

γ	Sc	Takhar et al [18]			Anderson et al. [10]			Present results		
		$n=1$	$n=2$	$n=3$	$n=1$	$n=2$	$n=3$	$n=1$	$n=2$	$n=3$
0.01	0.1	0.10306	0.10000	0.09857	0.0998	0.0959	0.0944	0.1026	0.0995	0.0983
0.1	0.1	0.15042	0.13077	0.12143	0.149	0.129	0.118	0.149	0.129	0.120
1.0	0.1	0.34940	0.28738	0.25085	0.348	0.286	0.249	0.34824	0.2860	0.249
10.0	0.1	1.01816	0.83237	0.72107	1.017 0.831	0.720		1.0168	0.83122	0.72011
0.01	1.0	0.59216	0.58844	0.58682	0.592	0.588	0.587	0.59135	0.58753	0.58602
0.1	1.0	0.67044	0.63724	0.62314	0.669	0.636	0.622	0.66898	0.63546	0.62136
1.0	1.0	1.17761	1.00100	0.90765	1.177	1.000	0.907	1.17650	1.000	0.90675
10.0	1.0	3.23257	2.64963	2.30414	3.232	2.649	2.303	3.23123	2.6485	2.3031

TABLE IV. Numerical values of wall shear stress $C_f\sqrt{\mathrm{Re}_x}$ and wall couple stress $g'(0)$ at $\beta = 3$ and $K = 0.2$ for various values of porosity parameter viscoelastic parameter and stretching/shrinking constant ε.

λ	ε	$k_0 = 0$		$k_0 = 0.05$		$k_0 = 0.2$	
		$C_f\sqrt{\mathrm{Re}_x}$	$-g'(0)$	$C_f\sqrt{\mathrm{Re}_x}$	$-g'(0)$	$C_f\sqrt{\mathrm{Re}_x}$	$-g'(0)$
0		1.63080	0.147704	1.69574	0.150151	1.96405	0.159666
0.2		1.78923	0.151601	1.85512	0.153961	2.12766	0.163149
0.4		1.93452	0.154952	2.00165	0.157247	2.27940	0.166188
0.6		2.06950	0.157894	2.13804	0.160139	2.42157	0.168884
0.8		2.19614	0.160515	2.26617	0.162721	2.55580	0.171304
1.0		2.31581	0.162880	2.38739	0.165052	2.68331	0.173500
2.0		2.83927	0.172108	2.91873	0.174169	3.24649	0.182153
3.0		3.28014	0.178721	3.36718	0.180712	3.72553	0.188401
5.0		4.01938	0.188007	4.12023	0.189906	4.53446	0.197195
10.0		5.44504	0.201486	5.57455	0.203239	6.10514	0.209909
0.5	-0.5	2.00316	0.156468	2.07098	0.158737	2.35157	0.167574
	-0.75	2.12000	0.180777	2.18940	0.183132	2.47034	0.192169
	-1	2.14165	0.203796	2.21416	0.206245	2.49578	0.215398
	0	1.55127	0.105704	1.61233	0.107628	1.87007	0.115249
	0.5	0.869310	0.0533198	0.910299	0.0545177	1.08586	0.059331
	0.75	0.456166	0.0267512	0.479693	0.58136	0.58136	0.030093
	1	0	0	0	0	0	0
	3	-4.92572	-0.217784	-5.42086	-0.228269	-8.02589	-0.274196

concentration field $\phi(\eta)$ for various values of the generative/destructive chemical reaction parameter γ and viscoelastic parameter k_0 with λ, K, k_0, Sc, n, β and ε are fixed. It can be seen from this figure that as γ increases from -1 to 1, we can find the decrease in the concentration field $\phi(\eta)$, whereas the concentration field increases with an increase in viscoelastic parameter k_0. Figure 11 describes the behaviour of the concentration field $\phi(\eta)$ for several values of the Schmidt number Sc and viscoelastic parameter k_0 in the case of destructive chemical reaction parameter ($\gamma = 2$ by keeping λ, K, n, β and ε fixed. From this figure we can see that with the increasing values of Sc dimensionless concen-

tration field $\phi(\eta)$ decreases while it increases by increasing the values of viscoelastic parameter k_0. Figure 12 depicts the variation of the Sherwood number or the rate of mass transfer at the wall $|\phi'(0)|$ versus the Schmidt number Sc for various values of the porosity parameter λ and the chemical reaction parameter γ by keeping K, k_0, n, β and ε fixed. From this figure it is evident that the magnitude of the Sherwood number is increased with an increase in both γ and λ.

Table II is made to show the numerical values of the skin-friction coefficient $C_f\sqrt{\mathrm{Re}_x}$ in the case of Newtonian fluid ($K = 0$, $k_0 = 0$) for different values of ε when the fluid flowing medium is not porous ($\lambda = 0$). From this table

we can see that the magnitude of the skin-friction coefficient $C_f \sqrt{\mathrm{Re}_x}$ decreases for $-0.24 \leq \varepsilon \leq 0$ and its value increases for $0 \leq \varepsilon \leq 5$. This table also gives the comparison of the present results for viscous fluid ($K = k_0 = 0$) and $\lambda = 0$ with the existing results of Bhattacharyya *et al.* [53], Wang [54], Ishak *et al.* [55] and Rosali *et al.* [56] and found to be in good agreement. Table III shows the comparison of numerical values of the Sherwood number $Sh_x(\mathrm{Re}_x)^{-1/2}$ for several values of γ, Sc and n in the case of Newtonian fluid ($K = k_0 = 0$) and $\lambda = 0$. From this table we found that the present results to be in excellent agreement with the results reported by Takhar *et al.* [18] and Anderson *et al.* [10]. Table IV gives the numerical values of skin-friction coefficient $C_f \sqrt{\mathrm{Re}_x}$ and wall couple stress g$'(0)$ for different values of λ, ε and k_0 with β and K are fixed. It can be seen from this table that the skin-friction coefficient and the wall couple stress are increased with an increase in both λ and k_0 (this can also see from Fig. 7 and 8). It is further noted that both the skin-friction coefficient and the wall couple stress are decreased and then increased for the values of $-0.5 \leq \varepsilon \leq 3$.

6.   Concluding remarks

The two-dimensional stagnation point flow of an electrically conducting micropolar viscoelastic fluid in a porous medium over a stretching/shrinking sheet in the presence of chemical reaction is investigated in this paper. The similarity transformations are used to convert the partial differential equations to a set of ordinary differential equations, and hence a analytical solution is obtained using homotopy analysis method. The fluid velocity, angular velocity and concentration profiles as well as local skin-friction coefficient, local wall couple stress and local Sherwood number are shown graphically and analyzed for various physical parameters of interest. From this study, we have made the following observations:

- The fluid velocity and angular velocity profiles are increased by increasing k_0 and λ whereas both are decreased with an increase in K.

- The skin-friction coefficient and wall couple stress increase by increasing K, k_0, and λ.

- It can also be concluded that the presence of Schmidt number and chemical reaction parameter is to decrease the concentration field whereas the presence of porosity parameter and rate of homogenous chemical reaction constant increases the concentration field.

- It is also observed that the presence of chemical reaction, Schmidt number and porosity medium is to increase the Sherwood number.

Acknowledgments

1. A.C. Eringen, *J. Math. Mech.* **16** (1966) 1-16.

2. A.C. Eringen, *J. Math. Anal. Appl.* **38** (1972) 480-496.

3. G. Lukaszewics, *Birkhäuser*, (Boston, MA, 1999).

4. A.C. Eringen, *Int. J. Eng. Sci.* **5** (1967) 191-204.

5. M.F. McCarthy, and A.C. Eringen, *Int. 1. Eng. Sci.* **7** (1969) 447-458.

6. S. De. Cicco, and L. Nappa, *Int. J. Eng. Sci.* **36** (1998) 883-893.

7. R. Kumar, *Int. J. Eng. Sci.* **38** (2000) 1377-1395.

8. R. Kumar, and S. Choudhary, *Proc. Indian Acad. Sci.* (Earth Planet. Sci.) **110** (2001) 215-223.

9. P.L. Chambre, and J.D. Young, *Phys. Fluids* **1** (1958) 48-54.

10. H.I. Anderson, O.R. Hansen, and B. Holmedal, *Int. J. Heat Mass Transf.* **37** (1994) 659-664.

11. R.A. Mohamed, and S. M. Abo-Dahab, *Int. J. Thermal sci.* **48** (2009) 1800-1813.

12. R. Cortell, *Chem. Eng. Process.* **46** (2007) 721-728.

13. R. Cortell, *J. Chem. Eng.* **46** (2007) 982-989.

14. U. N. Das, R. A. Deka, and V. M. Soundalgekar, *Forschung im Ingenieurwesen* **60** (1994) 284-287.

15. R. Muthucumaraswamy, *Acta Mech.* **147** (2001) 45-57.

16. R. Muthucumaraswamy, *Acta Mech.* **155** (2002) 65-70.

17. S.P.A. Devi, and R. Kandasamy, *Int. Commun. Heat Mass Transf.* **29** (2002) 707-716.

18. H.S. Takhar, A.J. Chamkha, and G. Nath, *Int. J. Eng. Sci.* **38** (2000) 1303-1314.

19. K.V. Prasad, S. Abel, and P.S. Datti, *Int. J. Non-linear Mech.* **38** (2003) 651-657.

20. R. Kandasamy, K. Periasamy, and K. Sivagnana Prabhu, *Int. J. Heat Mass Trans.* **48** (2005) 4557-4561.

21. Muhaimin, R. Kandasamy, and I. Hashim, *J. Nuclear Eng. Design* **240** (2010) 933-939.

22. P.K.Kameswaran, M. Narayana, P. Sibanda, and P.V.S.N. Murthy, *Int. J. Heat Mass Trans.* **55** (2012) 7587-7595.

23. K. Bhattacharyya, *Int. Commun. Heat Mass Trans.* **38** (2011) 917-922.

24. D. Pal, and S. Chatterjee, *Comm. Non-linear Sci. Numer. Simm.* **16** (2011) 1329-1346.

25. J.I. Oahimire, and B.I. Olajuwon, *J. King Saud university-Eng. Sci.* **26** (2014) 112-121.

26. D.W. Beard, and K. Walters, *Proc. Cambridge Philos. Soc.* **60** (1964) 667-674.

27. R. Nazar, N.A.D. Filip, and I. Pop, *Int. J. Non-Linear Mech.* **39** (2004) 1227-1235.

28. H. Xu, S.J. Liao, and I. Pop, *J. Non-Newtonian Fluid Mech.* **139** (2006) 31-43.

29. T. Hayat, T. Javed, and Z. Abbas, *Nonlinear Anal.: Real World Appl.* **10** (2009) 1514-1526.

30. Z. Abbas, Y. Wang, T. Hayat, and M. Oberlack, *Nonlinear Anal. Real World Appl.* **11** (2010) 3218-3228.

31. M. Sajid, Z. Abbas, T. Javed, and N. Ali, *Can. J. Phys.* **88** (2010) 635-640.

32. N.A. Yacob, A. Ishak, and I. Pop, *Comput. Fluids* **47** (2011) 16-21.

33. T. Hayat, Z. Abbas, and I. Pop, *Int. J. Heat Mass Transf.* **51** (2008) 3200-3206.

34. S.S. Mosta, Y. Khan, and S. Shateyi, *Math. Prob. Eng.* **2012** (2012) 290615.

35. S.K. Nandy, *Int. J. Eng. Math.* **2013** (2013) 187195.

36. S.M.M. El-Kabeir, *Can. J. Phys.* **83** (2005) 1007-1017.

37. Z. Abbas, M. Sheikh, and M. Sajid, *Can. J. Phys.* **92** (2014) 1113-1123.

38. Muhaimin, R. Kandasamy, I. Hashim, and A.B. Khamis, *Theo. Appl. Mech.* **36** (2009) 101-117.

39. V.K. Garg, and K.R. Rajagopal, *Acta Mech.* **88** (1991) 113-123.

40. G.S. Guram, and A. C. Smith, *Comput. Math. Appl.* **6** (1980) 213-233.

41. G. Ahmadi, *Int. J. Eng. Sci.* **14** (1976) 639-646.

42. Z. Abbas, Mariam Sheikh, and M. Sajid, *J. Porous media* **16** (2013) 619-636.

43. S.J. Liao, *Chapman & Hall/CRC Press*, (Boca Raton, 2003).

44. S.J. Liao, *PhD dissertation*, Shanghai Jiao Tong University, (1992).

45. S. Abbasbandy, *Phys. Lett. A* **360** (2006) 109.

46. T. Hayat, and Z. Abbas, *Z. angew. Math. Phys.* **59** (2008) 124-144.

47. Z. Abbas, Y. Wang, T. Hayat, and M. Oberlack, *Int. J. Nonlinear Mech.* **43** (2008) 783-793.

48. R. Abdoul Ghotbi, H. Bararnia, G. Domairry, and A. Barari, *Commun. Nonlinear. Sci. Numer. Simul.* **14** (2009) 2222-2228.

49. M.M. Rashidi, G. Domairry, and S. Dinarvand, *Commun. Nonlinear. Sci. Numer. Simul.* **14** (2009) 708-717.

50. Z. Abbas, Y. Wang, T. Hayat, and M. Oberlack, *Nonlinear Anual.: Real World Appl.* **11** (2010) 3218-3228.

51. Z. Abbas, and T. Hayat, *Numer. Mech. for PDE's* **27** (2011) 302-314.

52. M.M. Rashidi, S.A. Mohimanian pour, and S. Abbasbandy, *Commun. Nonlinear Sci. Numer. Simul.* **16** (2011) 1874-1889.

53. K. Bhattacharyya, S. Mukhopadhyay, and G.C. Layek, *Int. J. Heat Mass Transf.* **54** (2011) 308-313.

54. C.Y. Wang, *Int. J. Non Linear Mech.* **43** (2008) 377-382.

55. A. Ishak, Y.Y. Lok, and I. Pop, *Chem. Eng. Commun.* **197** (2010) 1417-1427.

56. H. Rosali, A. Ishak, and I. Pop, *Int. Commun. Heat Mass Transf.* **39** (2012) 826-829.